Thesis for the Degree of Master of Engineering

Synthesis and abrasion resistance of thermoplastic polyurethanes using hydroxyl-terminated polydimethylsiloxane and polyether polyols for 3D printers

by

Da-Bin Park
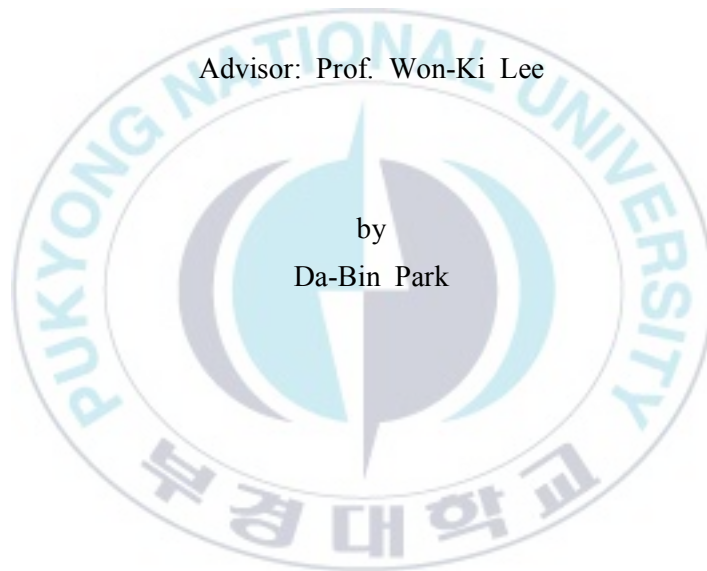
Department of Polymer Engineering

The Graduate School

Pukyong National University

February 21, 2020

Synthesis and abrasion resistance of thermoplastic polyurethanes
using hydroxyl-terminated polydimethylsiloxane and polyether
polyols for 3D printers
(폴리디메틸실록산 폴리올과 에테르계 폴리올을 이용한 3D
프린팅용 열가소성 폴리우레탄의 합성과 내마모특성)

Advisor: Prof. Won-Ki Lee

by
Da-Bin Park

A thesis submitted in partial fulfillment of the requirements for the
degree of Master of Engineering in Department of Polymer
Engineering, The Graduate School,
Pukyong National University

February 21, 2020

Synthesis and abrasion resistance of thermoplastic polyurethanes using hydroxyl-terminated polydimethylsiloxane and polyether polyols for 3D printers

A dissertation
by
Da-Bin Park

Approved by:

_____

(Chairman) Prof. Mun Ho Kim

_____

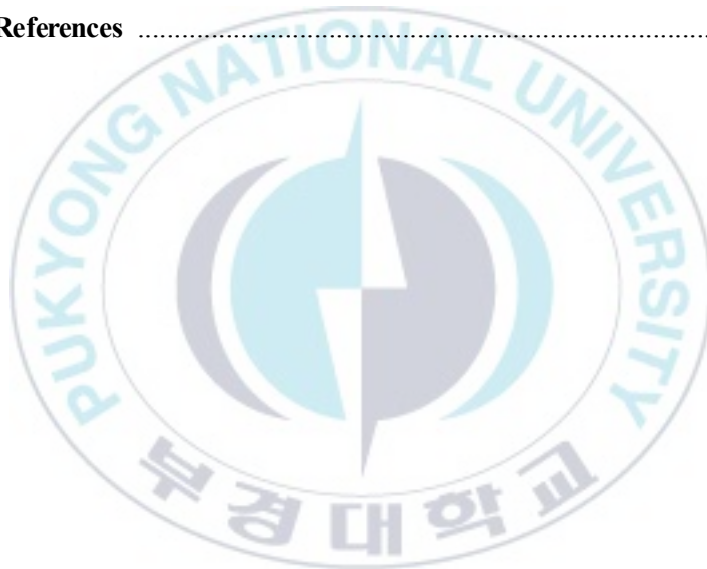(Member) Prof. Sang-Bo Park

_____

(Member) Prof. Won-Ki Lee

February 21, 2020

CONTENTS

List of Tables

List of Figures

폴리디메틸실록산 폴리올과 에테르계 폴리올을 이용한 3D 프린팅용 열가소성 폴리우레탄의 합성과 내마모특성

박다빈

부경대학교 대학원 고분자공학과

요   약

3D 프린팅 기술은 다품종 소량생산을 가능하게 하고, 최소한의 노동력으로 제품생산이 가능하므로 현재 빠르게 발전하고 있다. 3D 프린팅 방식은 SLA, SLS, FDM 등이 있으며, 그 중 FDM 방식은 재료를 필라멘트로 제조하여 필라멘트를 압출하는 방식으로 제품을 인쇄하는 방식이다. FDM 방식에서 기존에 자주 사용되는 재료는 ABS 수지와 PLA 수지가 대표적이다. 이 물질들은 고경도의 플라스틱으로 탄성이 거의 없어 생산할 수 있는 제품의 범위가 한정적이다. 이를 해결하기 위해 탄성과 기계적 물성이 우수한 열가소성 폴리우레탄을 필라멘트로 제조하여 3D 프린터에 적용하였다. 하지만 높은 탄성을 가지기 위해서는 저경도 타입의 폴리우레탄이어야 한다. 이 경우 내마모특성이 현저히 떨어지는 단점을 보인다. 본 연구에서는 저경도 타입의 열가소성 폴리우레탄의 내마모특성을 향상시키기 위해 양 말단이 수산기로 치환된 폴리디메틸실록산 폴리올을 추가로 사용하였다. 일반 폴리디메틸실록산의 경우 시간이 지남에 따라 제품의 표면으로 migration되어 표면이 미끌거리는 단점이 있지만, 수산기를 가지는 폴리디메틸실록산은 이소시아네이트와 반응해 우레탄기를 형성하여 사슬내부에 결합되어 migration을 방지한다. 폴리디메틸실록산 폴리올을 wt% 별로 첨가해 실험 하였고, 다른 물성들은 유지한 채 내마모성을 최대 향상시킬 수 있는 최적 함량은 5 wt%임을 알 수 있었다.

1. Introduction

Nowadays, 3D printing technology has revolutionized production techniques by enablingcomplex shapes to be produced using less material than traditional manufacturing methods[1]. Polymers for 3D printers include thermoplastics, thermosets, elastomers, hydrogels, functional polymers, polymer blends, and composites [2]. Among these, the thermoplastic polyurethanes (TPUs) can be used for various applications in a range of industries because their mechanical properties and glass transition temperatures can be controlled easily by adjusting the hard/soft segment ratio. For example, the polyurethanes (PUs) are used as shoe outsole materials instead of ethylene-vinyl acetate (EVA) elastomer and rubber [3] because the rebound resilience, which is an important property for shoe outsole material, can be optimized by adjusting the elasticity of the PU via the hard/soft segments ratio. In detail, an increase in the hard segments content for a given molecular weight leads to a decrease in the rebound resilience. In particular, PUs containing polyether display high rebound resilience [4-5].

In the previous study, we synthesized TPUs according to the hard

segment content for the production of 3D printing PU materials with high mechanical properties at low hardness. The results indicated that the highest strength was obtained with a hard segment content of 24 %, but at the cost of a reduction in abrasion resistance [6]. In the present study, TPUs were synthesized by adding a small amount of hydroxyl-terminated polydimethylsiloxane (PDMS-OH) in order to improve the abrasion resistance. This was informed by previous studies which demonstrated that the abrasion resistance was enhanced due to the low friction coefficient of PDMS, but that the migration of PDMS towards the surface led to the formation of TPU sheets and decreased the slip resistance over time [7-9]. To overcome this problem, the TPUs in the present study were synthesized using PDMS-OH instead of standard PDMS so that the hydroxyl groups could react with the isocyanate groups to incorporate the PDMS into the urethane main chains. The products were identified by Fourier transfer infrared spectroscopy (FT-IR) measurements during each synthetic step. After manufacturing the TPU sheets, the physical and thermal properties of TPUs with various PDMS-OH ratios were measured by differential scanning calorimetry (DSC),

thermogravimetric analysis (TGA), melt flow index (MFI), universal testing machine (UTM), rebound tester, and National Bureau of Standards (NBS) abrasion tester. In addition, nuclear magnetic resonance (NMR) spectroscopy, X-ray photoelectron spectroscopy (XPS), and contact angle measurements were used to demonstrate that the presence of PDMS-OH in the TPUs prevented the migration of PDMS to the surface.

2. Theoretical background

2.1. 3D printing

The rapid development and growth of 3D printing technology is presently outstripping those of most other technologies. 3D printing enables small quantities of customized goods to be produced at relatively low costs. Although the technique is primarily used to manufacture prototypes and mockups, a number of promising applications exist in the production of replacement parts, dental crowns, and artificial limbs, as well as in bridge manufacturing. The potential of 3D printing has been compared to such disruptive technologies as digital books and music downloads that enable consumers to order their selections online, allow firms to profitably serve small market segments, and enable companies to operate with little or no inventory of unsold finished goods. Some experts have also argued that 3D printing will significantly reduce the advantages of producing small lot sizes in low-wage countries by reducing the need for factory workers [10].

2.1.1. 3D printing technologies

  3D printing is an additive manufacturing (AM) technique for fabricating a wide range of structures and complex geometries from three-dimensional (3D) model data. The process consists of printing successive layers of materials that are formed on top of each other. 3D printing involves various methods, materials and equipment, has evolved over the years and has the ability to transform manufacturing and logistics processes. The technology was initially developed by Charles Hull in 1986 using a stereo lithography apparatus (SLA), with subsequent developments including powder bed fusion, fused deposition modelling (FDM), selective laser sintering (SLS) and polyjet printing. Additive manufacturing has been widely applied in different industries, including construction, prototyping and biomechanical devices [11]. The stereolithography apparatus (SLA) uses a vat of photopolymer resin which is activated by scanning the surface with a laser beam of UV light to form and shape each layer of the part. A piston then lowers the cured and formed layer into the vat, allowing the process to repeat and another layer of the part to be formed.

Although this older form of additive manufacturing provides the highest quality in terms of resolution and surface quality, the high cost is a disadvantage. In another example of additive manufacturing known as fused deposition modeling (FDM), the part is formed from a filament of polymer which is fed through a heated extruder nozzle and deposited on a build platform in successive layers. This method is cheap, user-friendly, fairly reliable, requires little post processing, and has experienced a boom in recent years with the availability of numerous desktop consumer models. However, disadvantages of FDM include warping, low surface quality, and low resolution. By contrast, selective laser sintering (SLS) primarily uses metals to form 3D parts, but post-processing treatments such as infiltration, sintering, and finishing, are required to complete the part. In this technique, metal powders are rolled across a build chamber and a laser or binder is directed into the powder to form the part layer. New powder is then rolled over the top of the layer, and the process repeats. Loose powder that is not formed into the part remains in the chamber to support the part as it is built. SLS is a low resolution method due to the limitations of the powder-based

material, which clumps at lower particulate sizes [12]. In the polyjet 3D printer, a carriage supporting four or more inkjet heads and ultraviolet (UV) lampstraverses the workspace and deposits tiny droplets of photopolymer materials which solidify when exposed to UV light. After printing a thin layer of material, the process repeats until a complete 3D object is formed.
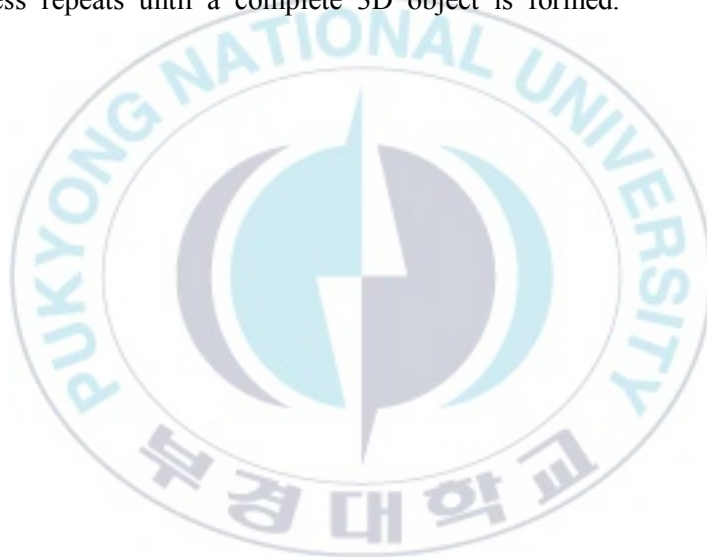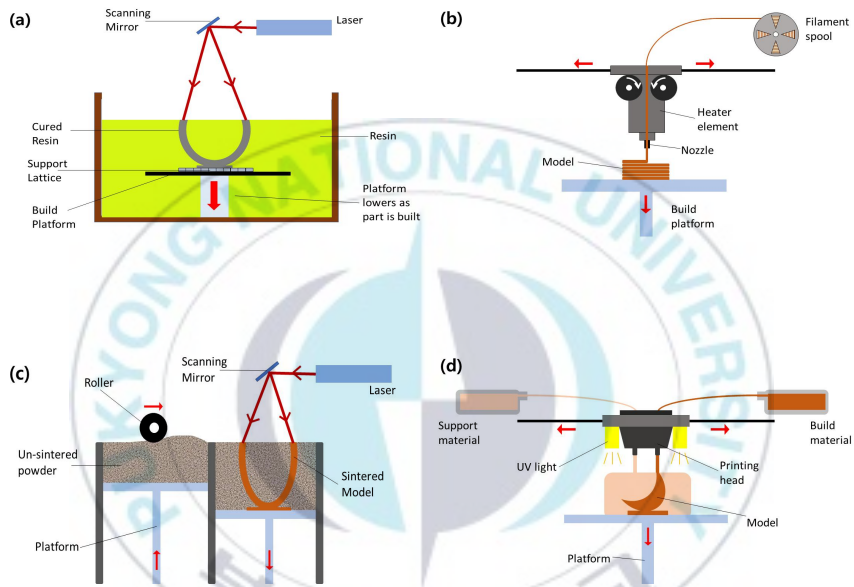
Figure 1. Methods of 3D printing : (a) Stereo lithography apparatus (SLA), (b) Fused deposition modeling (FDM), (c) Selective laser sintering (SLS), (d) polyjet

2.1.2. 3D printing materials

The choice of material depends on the 3D printing method. The stereolithography (SLA) technology involves the use of a photo-curable resin which is initially in the liquid state but becomes cured into the solid state by photopolymerization when exposed to a laser [13]. The fused deposition modeling (FDM) method uses a molten filament of thermoplastic resin to create objects by extrusion and deposition of the filament in layers [14]. While typical filament materials include poly(lactic acid) (PLA) and acrylonitrile-butadiene-styrene (ABS) resins, the characteristic stiffness of these materials places limitations on the products that can be manufactured. In the present work, a thermoplastic polyurethane (TPU) is suggested as an alternative material. The selective laser sintering (SLS) method is appropriate for a wide range of materials and applications. Almost any material can be processed, provided that it is available as a powder and that the powder particles can be sintered or fused when heated [15]. Similarly, the polyjet method makes use of a photo-curing polymer material [16].

2.2. Polyurethane

Polyurethane (PU) was originally discovered in 1937 by Otto Bayer and his co-workers at the laboratories of I.G. Farben in Leverkusen, Germany. Initial work focused on the realization of PU products obtained from an aliphatic diisocyanate and glycol. The poly(isocyanate) materials became commercially available in 1952 and was soon followed by the production of PU from toluene diisocyanate (TDI) and polyester polyols. In the years that followed (1952-1954), various polyester-poly(isocyanate) systems were developed by Bayer. The polyester polyols were gradually replaced by the polyether polyols with the advantages of low cost, ease of handling, and improved hydrolytic stability. The first commercially available polyether polyol, namely poly(tetrahydrofuran ether) glycol (PTMG), was introduced by DuPont in 1956 by the polymerization of tetrahydrofuran and, in 1957, BASF and Dow Chemicals produced the polyalkylene glycols, while DuPont produced a Spandex fiber named Lycra which was based on PTMG, 4,4'-diphenylmethane diisocyanate (MDI), and ethylene diamine. Over the subsequent decades, PU

evolved from flexible PU foams (1960) to rigid polyisocyanurate PU foams with good thermal resistance and flame retardance (1967) due to the emergence of several blowing agents, polyether polyols, and polymeric isocyanate such as poly methylene diphenyl diisocyanate (PMDI). The introduction of PU reaction injection molding (PU RIM) technology in 1969 was followed by further development into reinforced reaction injection molding (RRIM) which provided a high performance PU material and yielded the first plastic-body automobile in the United States in 1983. With the rising awareness of the hazards associated with the use of chloroalkanes as blowing agents (Montreal protocol, 1987), the 1990s saw the emergence of several other blowing agents in the market. At the same time, two-pack PU and PU-polyurea spray coating technology came to the forefront with the significant advantages of moisture-insensitivity and fast reactivity. This was followed by the emerging strategy of using vegetable oil-based polyols in the development of PUs. The present field of PU materials has developed considerably from PU hybrids, through PU composites, to non-isocyanate PU materials with versatile applications in a wide range of fields. Interest in PU materials

arose due to their simple synthesis (requiring few basic reactants), easy application protocol, and superior properties of the final product. The following sections provide a brief description of the raw materials required for PU synthesis and the general chemistry involved in its production [17].

2.2.1. Types of polyurethanes

The polyurethanes are present in every aspect of life and in many forms, from clothes and footwear, from furniture to roofing materials, from automobiles to construction [18]. Various types of polyurethane are available according to their synthetic route and applications. Commonly available polyurethanes are the low-density PU foams, which can be either rigid or flexible. The rigid foams have high mechanical strength, low heat conduction, low moisture absorption, and low density. Flexible foams are used for furniture, truck seating, and cushions [19]. Additionally, PU is used in the manufacturing of adhesives. Another type of PU is the PU elastomer, which can be regarded as a linear block copolymer. This segmented polymer structure can be provided with wide a range of properties, including various levels of stiffness and strength, by the modification of its three basic building blocks, namely: the polyol, diisocyanate and chain extender. The consequent range of hardness extends from that of a soft jelly-like structure to the hard rigid plastics. The properties are related to segmented flexibility, chain entanglement, interchain forces, and

crosslinking [20]. While the PU elastomers are generally thermosetting, thermoplastic polyurethanes (TPUs) also show outstanding versatility, with a wide range of physical properties being accessible through the suitable choice of diols and di-isocyanates in their synthesis [21]. Since the aim of the present work is to examine TPUs for use in a 3D printer filament, all the experiments and analyses will focus specifically on this type of material.

POLYURETHANES

Thermoplastic PU	Flexible PU	Rigid PU	PUI	Water-borne PU
Examples: Keyboard protector for laptop, outer cases of mobile electronic devices, automotive instrument panels, caster wheels, power tools, sporting goods, medical devices, drive belts, footwear, inflatable rafts, and a variety of extruded film, sheet and profile applications.	Examples: Cushion materials, carpet underlays, furniture, bedding, automotive interior parts, packaging, biomedicine and nanocomposites	Examples: Thermal and sound insulators	Examples: Artificial hearts, connector tubing for heart pacemakers and haemodialysis tubes	Examples: Coatings, adhesives, sealants, binders

Figure 2. Industrial application fields of polyurethane [22]

2.2.2. Structure of polyuretane

The polyurethane structure is divided into soft segments consisting primarily of polyols and hard segments composed mainly of di-isocyanates, chain extenders, and urethane and urea bonds. The hard segments contain strongly polar urethane bonds which facilitate the formation of strong links with adjacent hard segments to produce an aggregate structure. In contrast, the soft segments are hydrophobic and form an amorphous, flexible chain. The polar hard segment and the hydrophobic soft segment are therefore phase-separated, forming the structure shown in **Figure 3**. In TPU, this phase separation leads to the formation of domains in which the hard segments serve as crosslinks between the amorphous polyester or poly ether soft segments. The hard segment domains are crystalline and there has been considerable interest in the contributions of hydrogen-bonding and chain-packing towards the structural stability [23].
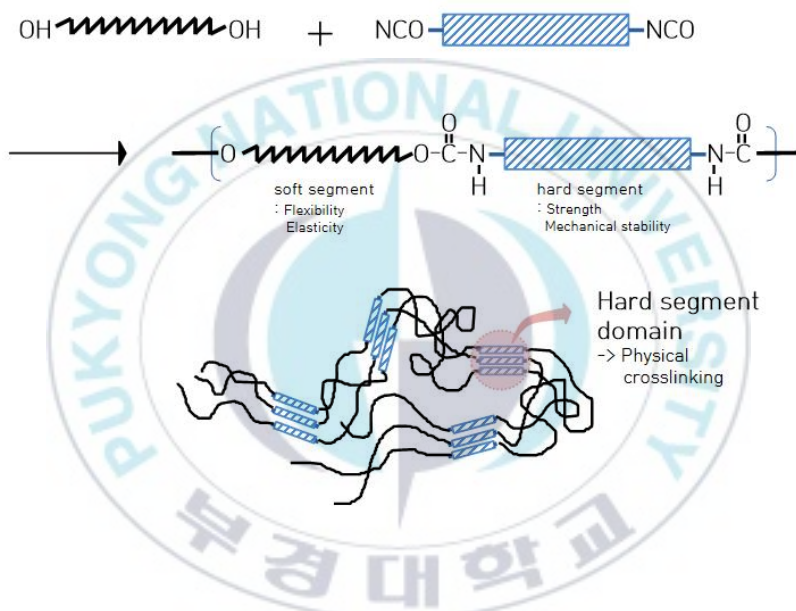
Figure 3. Structure of hard domain & soft domain in polyurethane

2.2.3. Base materials

2.2.3.1. Polyols

The polyols are a major component of the soft segment in the PU structure and have a great influence on properties such as flexibility and elasticity. The raw materials used in the synthesis of PU generally contain multiple hydroxyl, carboxyl, and amine groups, with the term polyol specifically referring to the multiple hydroxyl groups. The hydroxyl-containing polyols can be classified into three types, namely the polyesters, polyethers, and others **(Table 1)**. The polyester polyols contain an ester (-COO) group in their structure and are produced by a condensation reaction between a glycol and a dibasic acid. The superior characteristics of polyester polyol based PUs are explained by an enhanced crystalline structure in the urethane segment [24, 25]. They have superior thermal, fire-resistant, and solvent-resistant properties compared to the polyether-based PUs due to the strong secondary forces between the polyester chains [26]. However, the polyester polyols have the disadvantage of being hydrolyzed by water. The

polyether polyols are produced by the polymerization of ethylene oxide and propylene oxide in the presence of an alkaline catalyst and are more flexible than the polyester polyols in terms of bonding structure. Although the polyether polyols display low abrasion resistance [27], the present work demonstrates the increased abrasion resistance of the polyether-based TPUs. The remaining polyols, listed under "others", include the polycarbonates, polybutadienes, acryls, and non-flammable polyols.
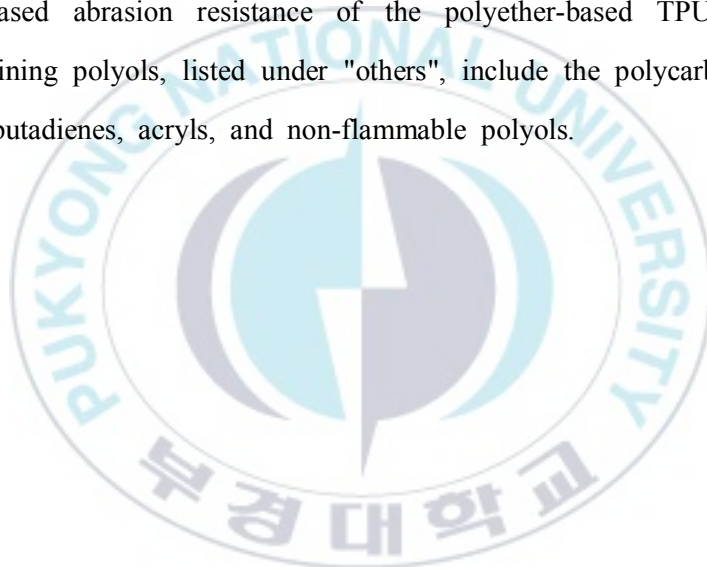
Table 1. Various kinds of polyol

Types	
Polyether Polyol	PPG (Polypropylene Glycol)
	PPG denaturant
	PTMG
Polyester Polyol	Poly condensation polyester polyol (Adipate)
	Ring-opening polymerization polyester polyol (Lactone)
The other types polyol	Polycarbonate Polyol
	Polybutandiene Polyol
	Acryl Polyol
	Non-flame Polyol

2.2.3.2. Isocyanates

The isocyanates used industrially contain two or more NCO groups that react with a polyol to form a urethane bond. Wurtz (1848) and Hentchel (1884) presented a method for synthesizing isocyanates and in 1937 Otto Bayer was the first to synthesize the di-isocyanates. The isocyanate compound is a major component of the hard segment of the PU structure and has a great influence on the mechanical properties such as strength and hardness. The basic properties of the main isocyanate compounds are presented in **Table 2**. The isocyanates are broadly divided into the aromatic and aliphatic isocyanates. While the aromatic isocyanates are more reactive than the aliphatic isocyanates, the formation of chromophores in the benzene ring causes yellowing and relatively poor light stability. In the present work, the aromatic isocyanate methylene diphenyl diisocyanate (MDI) is used due to the need for a rapid reaction with the chain extender during TPU production.

Table 2. Properties of isocyanate compounds

Property		2,2 MDI	4,4 MDI	2,4 MDI	2,4 TDI	2,6 TDI	HDI	IPDI	H12 MDI
physical state		Solid	Solid	Solid	Liquid	Liquid	Liquid	Liquid	Liquid
Color		white to pale yellow			colorless to pale yellow		colorless	colorless	colorless
Odour		none. pungent at high temperature			characteristic, sharp, pungent		pungent		
Molecular weight		250.3			174.2		168.2	222.3	262.35
Melting point, ℃		46	40	36	21.8	18.2	-67	-60	78-82
Boiling point, ℃	0.07 kPa	142	161	152			96-110		155-166
	1.33 kPa				120		127	158	
	101 kPa		314		251		255		
Flash point, ℃			212-214				130-140	100	>200

- 22 -

2.2.3.3. Chain extenders

During the synthesis of polyurethane, the activity of the growing chain becomes weaker, and the reaction with other monomers more difficult, as the molecular weight increases. Therefore, in order to obtain a high molecular weight polyurethane, a low molecular weight bi-functional compound (a diol or diamine) is added as a chain extender, while tri-functional or higher functional compounds are used as cross-linking agents. The various combinations of chain extenders and cross-linking agents are presented in **Table 3**. Since the mechanical properties and thermal stability of the obtained polyurethane are determined by the structure and length of the chain extender [28], the appropriate chain extender is selected according to the intended application.

Table 3. Types of chain extenders

Types	Chain extender & Cross linking agent
Diol	Ethylene Glycol Propylene Glycol 1,4-butandiol
Triol	Glycerine Trimethyol propane
Tetraol	Pentaerythritol Oxypropylated ethylene diamine
Diamine	Hexamethylenediamine m-Phenylenediamine
Aminoalcohol	Diethanolamine, DEOA Triethanolamine, TEOA

2.2.4 Polymerization of TPU

Polyurethane refers to a polymer with a main chain of urethane bonds formed by the reaction of a hydroxyl group and an isocyanate group. The reaction mechanism, termed poly-addition, is similar to condensation polymerization with the distinction that no by-products are generated. In the present study, TPUs were polymerized in two steps. First, the NCO-prepolymer was synthesized by the reaction of a polyol with an isocyanate having a higher molar ratio. The percentage of remaining NCO groups of the isocyanate (theoretical value) was calculated by the following equation :

$$\% \ NCO = \frac{NCO \ (g) \ value}{Total \ reactant \ weight \ (g)} \times 100 \ (\%)$$

where $\% \ NCO$ is the specific rate of isocyanate functions, that is, the mass percentage of available isocyanate functions relative to the mass of analyzed MDI. The change in NCO value during the reaction was then determined by the dibutylamine (DBA) back-titration method. When the theoretical value was reached, the

reaction was terminated, and the remaining isocyanate was reacted with the chain extenders in the second step to produce the TPU resin.
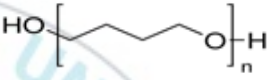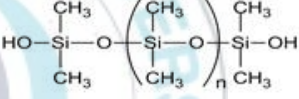
2.3. Polymer processing
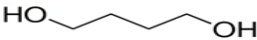
In order to use a polymer as a commercial product, it is necessary to perform a processing procedure after synthesis. This procedure determines the crystallinity and orientation of the polymer. The emphasis of polymer processing is to satisfy the requirements of high-quality materials for the design of molds, machinery and products at competitive prices. Polymer processing is divided into casting, injection molding, compression molding, extrusion, blow molding, calendering, lamination, rotational molding, and thermoforming techniques and can be used to generate products such as fibers, filaments, and films.

3. Experimental

3.1. Materials

To synthesize TPU, polyether polyol (Mw = 3200 g/mol, Daewon Polymer Co., Ltd.) and hydroxyl-terminated polydimethylsiloxane (PDMS-OH, Mw = 1800 g/mol, Wacker Chemical Co., Ltd.) were used. 4,4'-Diphenylmethane diisocyanate (MDI, Mw = 250.26 g/mol, Aldrich Chemical), which is an aromatic isocyanate, was used without purification. 1,4-butanediol (1,4-BD, Mw = 90.12 g/mol, Aldrich Chemical) was employed as chain extender.

Table 4. Information on reagents used in this study

| Name	Molar Weight (g/mol)	Melting Temp (℃)	Boiling Temp (℃, 1 atm)	Structure
Poly (tetrahydro furan)	2900	30~43	-	
PDMS-OH	1800	-40	280	
MDI	250.25	40	314	
1,4-Butanediol	90.12	16	230	

3.2. Synthesis of Thermoplastic polyurethane

Polyether polyol and hydroxyl-terminated PDMS were degassed at 90 ℃ in a vacuum pump before use. They were weighted and added to a 1000 mL four-necked reactor equipped with a thermometer, a stirrer, and a nitrogen inlet, where they were homogeneously mixed at 85 ℃ for 1 hr **(Figure 4)**. Then, MDI was added and mixture was left to react at 85 ℃ for approximately 3 hr under moderate stirring (60~70 rpm). The synthesis of NCO-terminated prepolymer was confirmed by using the dibutylamine (DBA) back-titration method (ASTM D 1638), and the prepolymer was synthesized by allowing the reaction to proceed until the theoretical NCO content was reached. The synthesis of NCO-terminated prepolymer was degassed at 90 ℃ in a oven. Then, the prepared prepolymer and 1,4-butanediol (1,4-BD) were weighted and the mixture was reacted to chain extender reaction for approximately 2~3 min under stirring (1000 rpm). The completely synthesis of TPU was poured on a teflon sheet and stored at 90 ℃ in a oven for 1 day. The reaction compositions and scheme are shown in **Table 5** and **Figure 5**, respectively.
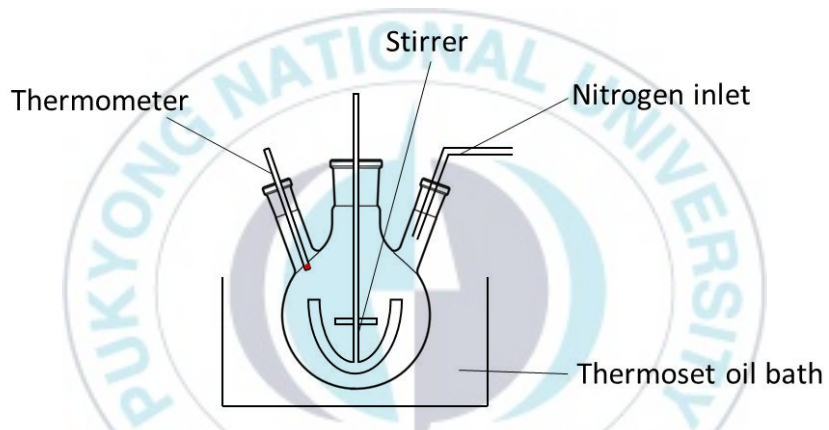
Figure 4. Synthetic tools for synthesis of NCO-prepolymer

Table 5. Composition and characterization of TPUs

Sample	Molar ratio				Hard Segment (%)	Hardness (shore A)	PDMS ratio (wt%)
	Poly ether diol	PDMS-OH	1,4-BD	MDI			
TPU-0	0.35	-	0.65	1.05	24	71	0
TPU-1	0.34	0.005	0.65	1.05	24	71	1
TPU-5	0.33	0.022	0.65	1.05	24	70	5
TPU-10	0.30	0.043	0.65	1.05	24	62	10
TPU-20	0.26	0.086	0.65	1.05	24	62	20
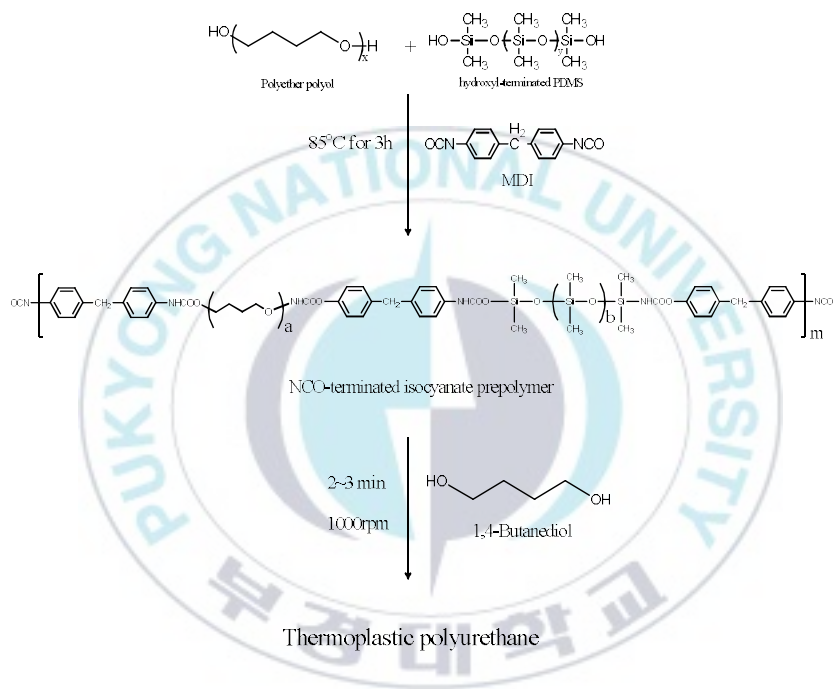
Figure 5. Synthetic process of TPU

3.3. Manufacture of TPU filament for 3D printing

The TPU resin was manufactured in the form of a TPU sheet using a press machine at 180 ℃ for 10 min. The mechanical properties of the TPU sheets were then measured. Finally, the TPUs were extruded into filaments for use in 3D printers as shown in **Figure 6**.
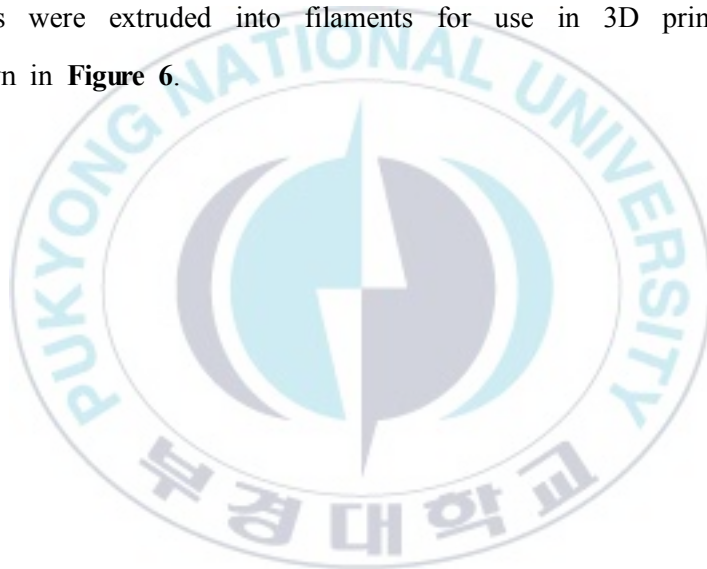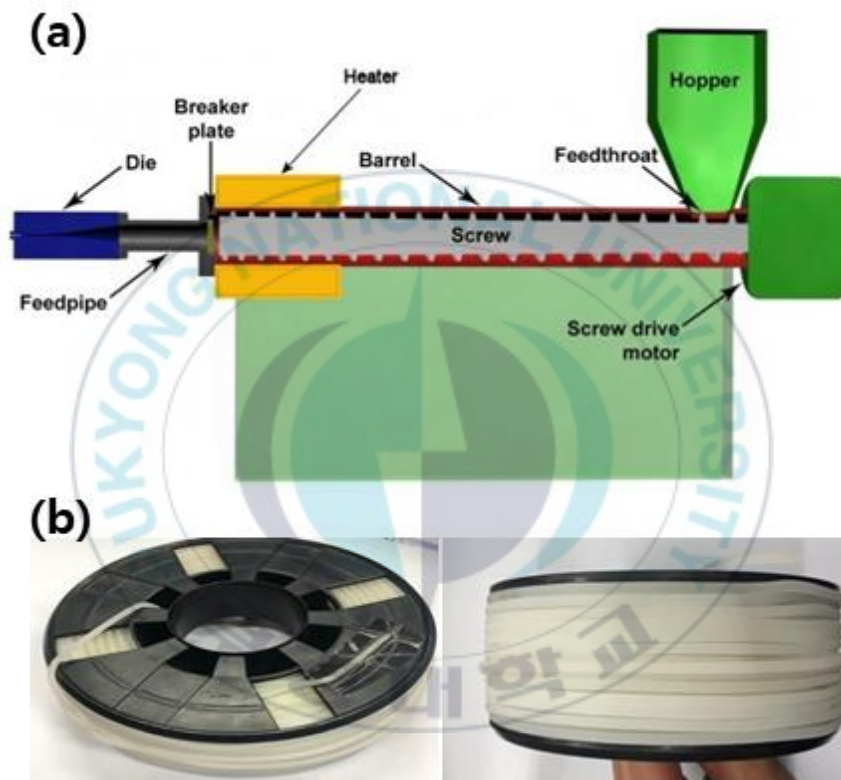
Figure 6. (a) Illustration of filament extruder, (b) TPU based filament manufactured by extruder

3.4. Characterization

FT-IR spectroscopy (FT-IR, Jasco 430) was used to identify both PDMS-OH react to urethane reaction and each synthetic step of polyurethane. For each IR spectrometer sample, 32 scans at a 4 cm^{-1} resolution were collected in the transmittance mode. And the spectra were analysed in the wavelength range of 4000-400 cm^{-1}. The thermal property of the TPUs was measured using differential scanning calorimetry (DSC, TA instrument Q-100) at a heating rate of 10 ℃/min from -80 ℃ to 250 ℃. And, The thermal stability of TPUs were measured by thermogravimetric analyzer (TGA Q500 instrument) in a range from 80 ~ 800 ℃ using a heating rate of 10 ℃/min in N_2 atmosphere. The tensile strength tests of TPUs were measured using a UTM (Daesung tester, DTU-900HMA). The samples of TPUs were manufactured dumbbell shape with a thickness of 0.2 ± 0.03 cm and width of 0.5 cm according to ASTM D 412. The test speed was 500 mm/min, and the tests were repeated five times to obtain the average value. In NBS abrasion test, three samples with thickness 6.3 mm were abraded across the surface of a rotating, abrasive drum until 2.54 mm of

the sample was abraded. A rubber standard was tested before the test. Based on the cycles to abrade the sample and the rubber standard. NBS abrasion resistance was then calculated according to ASTM D 1630-16. The slip resistance was tested as friction coefficient test using a UTM according to ASTM D 1630-16. The rebound resilience was measured using rebound resilience tester (WITHLAB Co., WL1300) and the samples were prepared to 5 layers according to ASTM D 3574. The inhibition of migration of PDMS were demonstrated by nuclear magnetic resonance (NMR) and X-ray photoelectron spectroscopy (XPS).

4. Results and discussions

4.1. Analysis of prepolymer

4.1.1. Free-NCO %

The free-NCO% value is important for monitoring the progress of an NCO-prepolymer synthesis, providing an indication of the content of unreacted isocyanate (NCO) groups in the total reactants. **Table 6** presents the theoretical free-NCO% values of each TPU sample along with an example calculation. During synthesis, the experimental value of the NCO content is measured using the dibutylamine (DBA) back-titration method (**Figure 7**) and compared with the theoretical value to determine whether to terminate the reaction. The experimental values of the NCO content were calculated by the following equation:
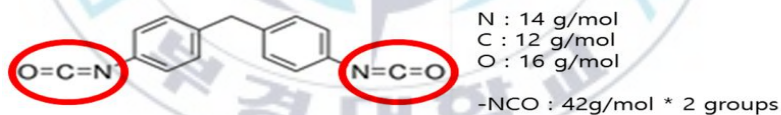
$$\frac{(B-A) \times f \times 0.042}{W} \times 100 \ (\%)$$

where B = blank value (ml), A = titration amount of HCl (ml), f = titer of 1N HCl, and W = total weight of reactants (g). When the experimental value was equal to the theoretical NCO content, the chain extenders were added to the NCO-prepolymer and the available NCO groups were fully consumed by the chain extending reaction.

Table 6. Theoretical values of free-NCO% and an example of calculating of value of the TPUs

sample	Total wt of reactants (g)	isocyanate (mol)	diol (mol)	Free-NCO %
TPU-0	1278	1.05	0.35	4.60 %
TPU-1	1264	1.05	0.35	4.65 %
TPU-5	1275	1.05	0.35	4.61 %
TPU-10	1282	1.05	0.35	4.59 %
TPU-20	1295	1.05	0.35	4.54 %

O=C=N — [benzene] — CH₂ — [benzene] — N=C=O

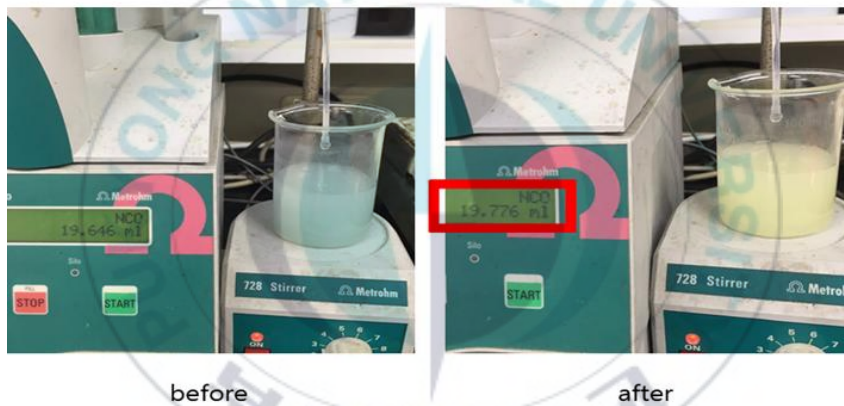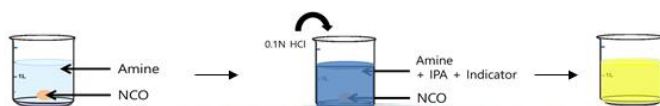N : 14 g/mol
C : 12 g/mol
O : 16 g/mol

-NCO : 42g/mol * 2 groups

- remained isocyanate (mol) : isocyanate − diol

EX) TPU-1 (Total wt : 1264 g)

remained isocyanate (mol) : 1.05 − 0.35 = 0.7

[(2 * 42g/mol * 0.7mol)/ 1264 g] * 100%

= 4.65 %

Figure 7. Process of NCO back-titration

4.2. Analysis of thermoplastic polyurethanes

4.2.1. FT-IR spectra

The synthesis of TPU was monitored by FT-IR spectra. **Figure 8** shows FT-IR spectra of polyol mixture of polyether diol and PDMS-OH, prepolymer, and TPU. The spectrum of the mixture in Figure 8(a) shows broad absorption peaks at 3200-3550 cm^{-1}, which are from the stretching of terminal -OH groups. Additionally, the diol mixture showed the characteristic peaks, -CH$_3$ stretching at 2970cm^{-1}, -C-O-C- stretching at 1140 cm^{-1}, and -Si-O-Si- stretching at 1067 cm^{-1}. Figure 8(b) shows the spectrum of the prepolymer which mainly characterized by the peaks of urethane bond at 1500 cm^{-1} (-C-NH- stretching) and 1700 cm^{-1} (-COO- stretching). Furthermore, the NCO peak of the unreacted MDI was observed at 2270 cm^{-1}. From Figure 8(c), TPU with PDMS was successfully synthesized because the -NCO stretching peak was clearly disappeared.
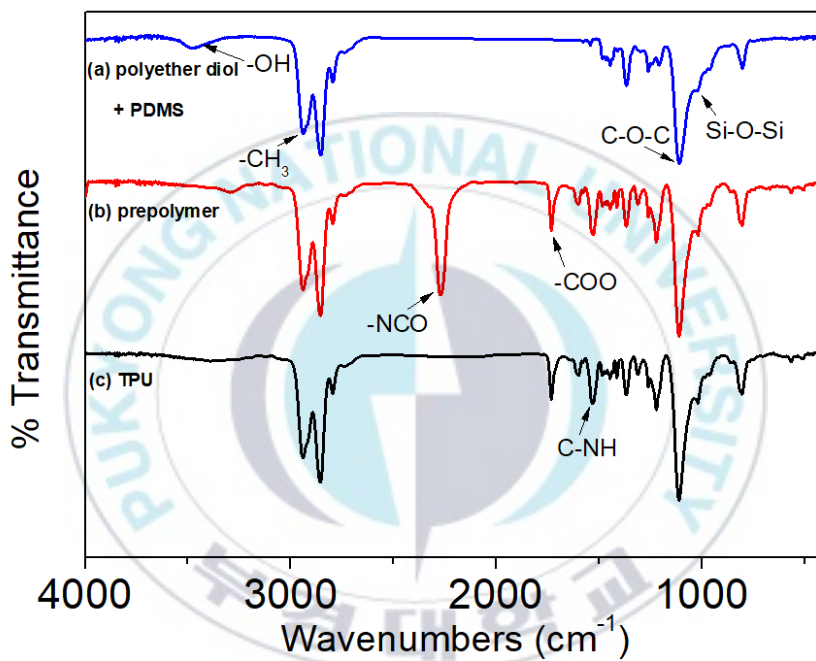
Figure 8. FT-IR spectra of TPU : (a) polyol mixture, (b) prepolymer, and (c) TPU

4.2.2. Thermal properties

4.2.2.1. Differential scanning calorimetry (DSC)

The thermal property of TPUs with different compositions of polyols was investigated by DSC (**Figure 9**). The glass transition temperatures (T_g) of TPUs with 0, 1, 5, 10, and 20 wt % of PDMS-OH are –73.8 ℃, -74.3 ℃, -74.6 ℃, -74.9 ℃, and –76.2 ℃, respectively. As the content of PDMS-OH increases, T_g decrease marginally from –73.8 ℃ to –76.2 ℃. T_g is affected by the siloxane groups of the PDMS-OH. If the degree of phase separation is decreased, T_g of soft segment is decreased because the hard segment domain is more stiff than soft one and then the soft segment domain is influenced by the hard one [29]. And, the PDMS have soft characteristic. The PDMS is hydrophobic and then the introduction of PDMS results in the decrease of degree of phase separation. Therefore, T_g from polyether diol decreases with increasing content of PDMS-OH. T_g, T_c, and T_m are shown in **Table 7**.
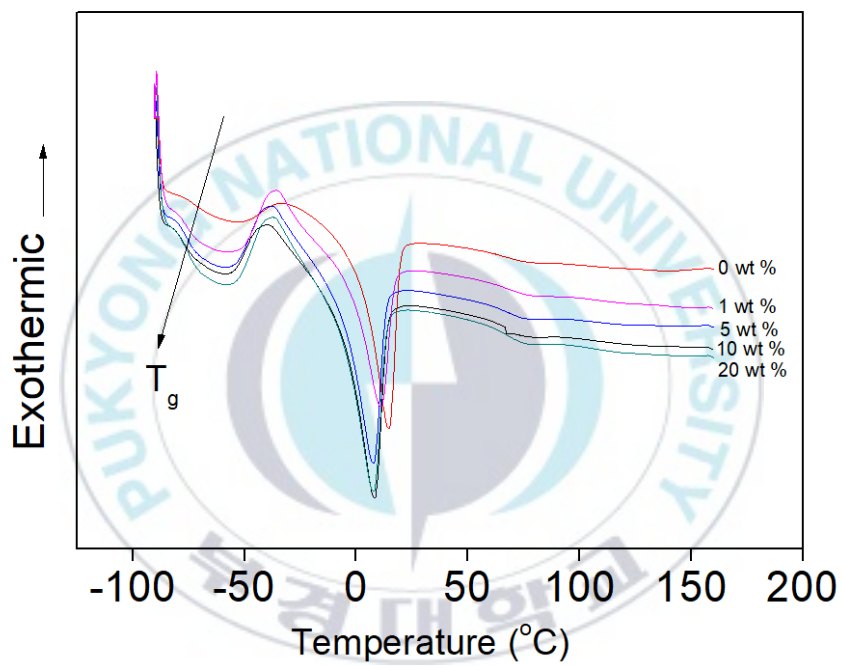
Figure 9. DSC thermograms of TPUs with 0, 1, 5, 10, and 20 wt% of PDMS

Table 7. T_gs, T_cs, and T_ms of the TPUs with PDMS-OH wt%

Sample	TPU-0	TPU-1	TPU-5	TPU-10	TPU-20
T_g (℃)	-73.8	-74.3	-74.6	-74.9	-76.2
T_c (℃)	-23.9	-24.7	-25.1	-32.4	-33.2
T_m (℃)	17.2	13.1	13.2	18.6	14.9

4.2.2.2. Thermogravimetric analysis (TGA)

Since the TPU-based filaments are used in the FDM method, which prints by extrusion through a high-temperature nozzle, it is necessary to know the heat deflection temperature of the resin and to set the temperature of the nozzle accordingly. The starting temperature of pyrolysis of the synthesized TPU was therefore confirmed by thermogravimetric analysis (TGA). As indicated in **Figure 10**, pyrolysis of the TPU-5 sample began to cause marginal degradation at around 300 ℃. It is therefore concluded that this sample can be used at temperatures below 300 ℃.
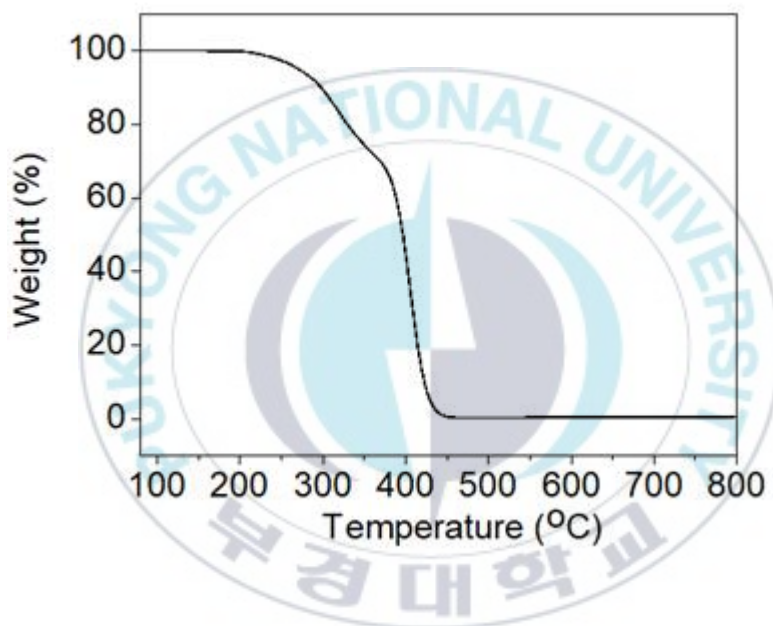
Figure 10. TGA curve of TPU with 5 wt% of PDMS-OH

4.2.2.3. Melting flow index (MFI)

The melting flow index (MFI) indicates the ease of flow of the melt at the flow rate when the thermoplastic polymer melt is extruded from the piston under a given set of conditions (unit: g/10min). A low MFI value indicates a low flow of resin; hence, appropriate MFI values are necessary for use in 3D printers employing the FDM method. In general, the nozzle temperature of FDM machines can tolerate high temperatures above 300 ℃. Most resins will melt well and provide a high MFI value at such temperatures, so that there will be no problem in proceeding with excellent flowability. However, if the temperature is too high, it may cause thermal degradation of the resin (**Figure 11**). Therefore, based on the TGA results, materials that melt well at temperatures below 300 ℃are suitable for FDM because they do not suffer thermal degradation at those temperatures. The commercialized filament (INKRAYON, KOLON PLASIC Inc) displays an MFI value of 12 - 16 g/min at around 240 ℃. Hence, if the manufactured TPU displays a similar MFI value to the commercial filament at 240 ℃, it is considered to be a suitable material for

the FDM method. The results presented in **Figure 12** indicate that, at 190 ℃, the MFI values of the TPUs were too low for use in FDM methods. However, at 240 ℃(which is below the heat degradation temperature) the MFI values of all the samples are comparable to those of commercial INKRAYON filaments. Hence, the TPUs with PDMS-OH are appropriate for use in the FDM methods of 3D printing at 240 ℃.
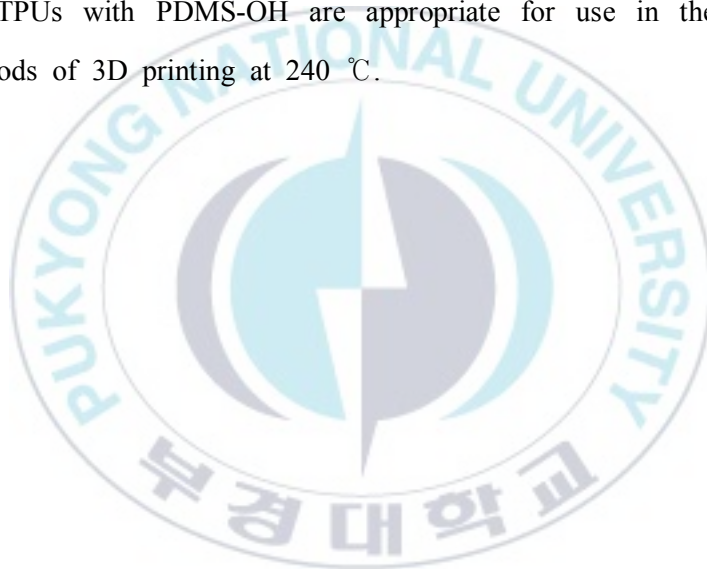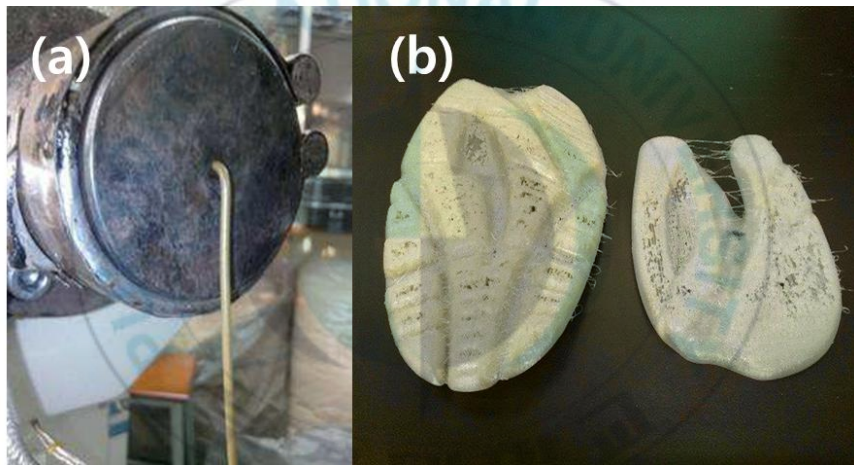
Figure 11. Images of thermal deformation of TPU : (a) at the extruder machine [30], (b) at the printing model
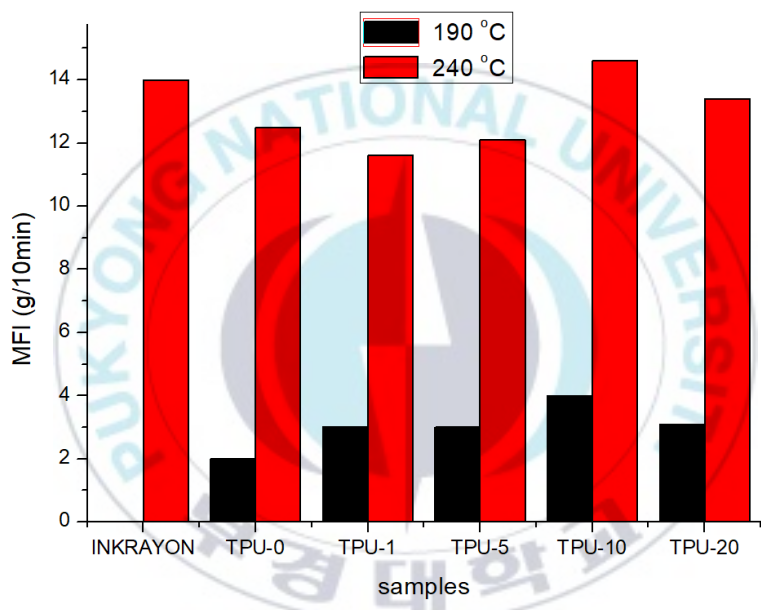
Figure 12. MFI values compared INKRAYON with TPUs

4.2.3. Nuclear magnetic resonance (NMR)

NMR spectra were acquired in order to identify the molecular structure of the synthesized TPUs with PDMS-OH and the relative amounts of C, O, N, and Si. The ^{1}H-NMR spectrum of the sample TPU-1 and its structure are presented in **Figure 13**. The peaks at ca. 0.1, 1.6, 3.4, 4.2, and 7 ppm correspond to -(CH$_3$-Si-CH$_3$)-, -(CH$_2$)-(polyol), -CH$_2$-O-, -(CH$_2$)-(MDI), and the H atoms of the benzene rings, respectively. These peak assignments indicate that the TPUs were successfully synthesized and gives a measure of the total atoms content ratio of the TPUs.
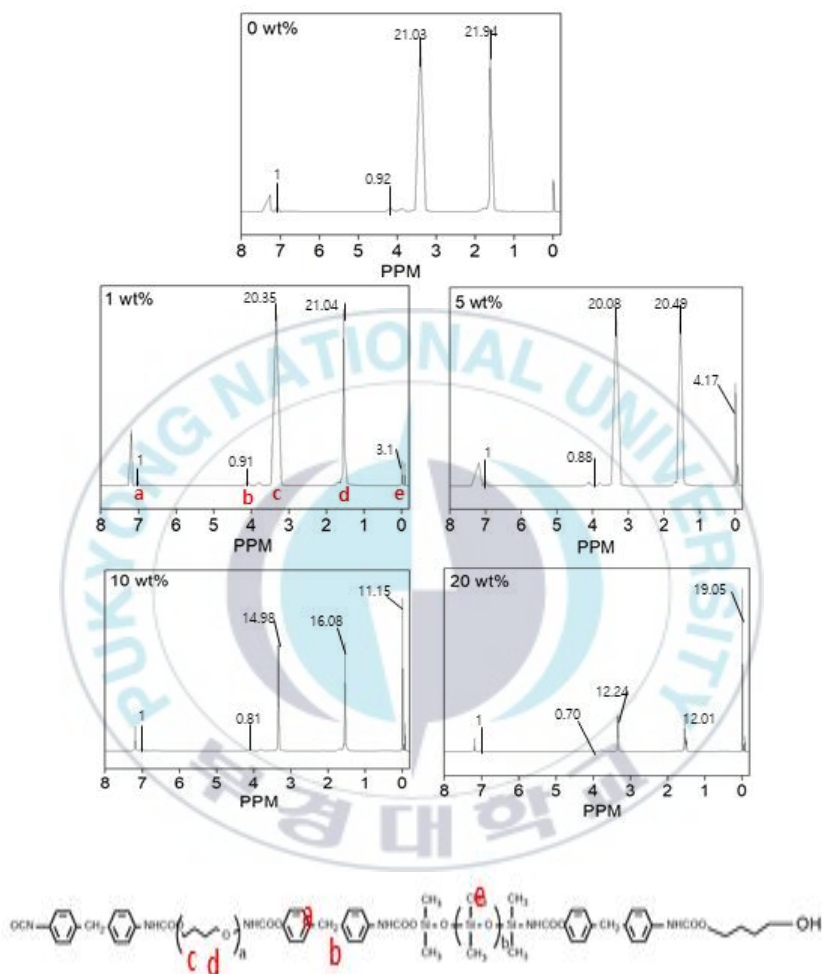
Figure 13. ^{1}H-NMR spectra and element content ratio of the TPUs with 0, 1, 5, 10, 20 wt% of PDMS-OH

4.2.4. Surface properties

4.2.4.1. X-ray photoelectron spectroscopy (XPS)

The survey spectra of each TPU surface presented in **Figure 14** indicate that TPU-0 consists of atoms of carbon, nitrogen, and oxygen, while the others display two additional small peaks, Si_{2s} and Si_{2p} due to the presence of PDMS. As the proportion of PDMS-OH in the TPU increases, the ratio of Si increases and the ratio of C decreases due to the decrease in the proportion of ether polyol. Although PDMS generally migrates towards the surface due to its low surface energy and hydrophobic properties, the aim was to prevent this by introducing the urethane bond in PDMS-OH.
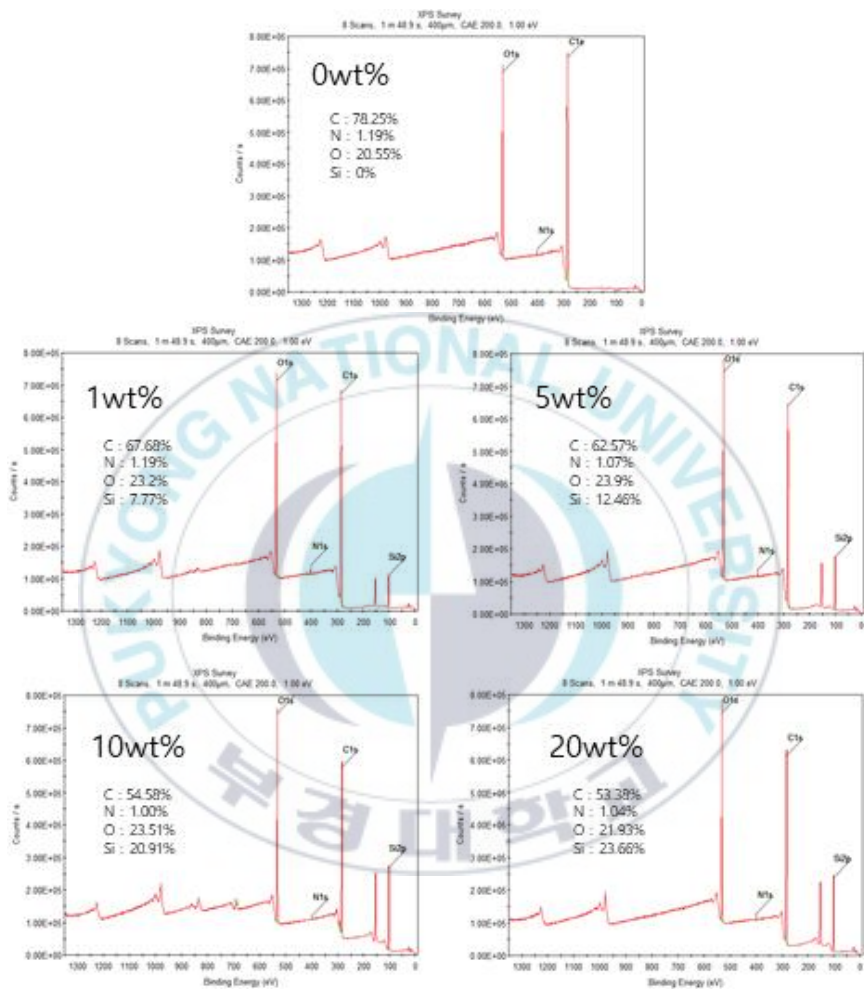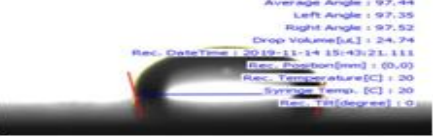
Figure 14. XPS spectra of each surface of the TPUs with 0, 1, 5, 10, 20 wt% of PDMS-OH

4.2.4.2. Contact angle

Since the PDMS has a high hydrophobicity, migration of the PDMS-OH towards the surface of the TPU sample would increase the contact angle with water compared to that of the TPU in the absence of PDMS. The migration behaviors of the normal PDMS and the PDMS-OH in the TPU are presented in **Figure 15** and the contact angle at each PDMS-OH content is presented in **Figure 16**. It can be seen that although the contact angles did not show much difference in the presence of 0, 1, and 5 wt% PDMS, an increase in contact angle occurred in the presence of 10 and 20 wt.% PDMS due tothe inhibition of migration by the urethane linkages. However, delocalization of the excess PDMS occurred at above 10 wt% PDMS.
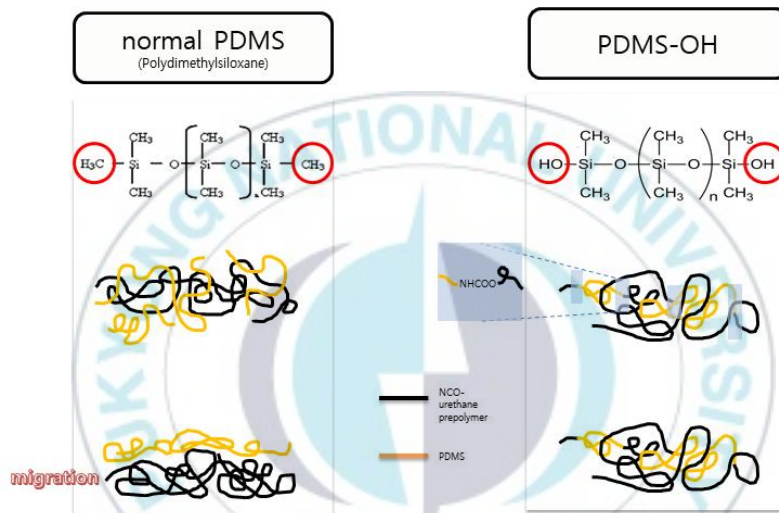
Figure 15. Behaviors of PDMS and PDMS-OH in the TPU

PDMS-OH (wt%)	image	Contact angle (°)
0 (none)		Left : 68.62 Right : 68.62
1		Left : 68.18 Right : 68.10
5		Left : 70.40 Right : 70.48
10		Left : 96.35 Right : 95.61
20		Left : 97.35 Right : 97.52

Figure 16. Contact angles of TPUs with water

4.2.4.3. Total reviews of surface properties

The NMR and XPS spectra were compared in order to identify the migration of PDMS in the TPUs. The total and surface atom ratios of each TPU are indicated by the respective atom ratios in each of the NMR and XPS spectra. The total and surface Si/C ratio of each TPU are presented in **Table 8** and **Figure 17**. Migration of the PDMS to the surface would be expected to lead to an increase in the surface Si/C ratio with increasing wt% of PDMS. However, the total and surface Si/C ratios of the TPUs are seen to be similar at each wt%, clearly indicating that migration of the PDMS was prevented. In addition, while migration of the hydrophobic PDMS would lead to a greatly improved contact angle at a small amount (1 wt%) of TPU, no significant difference in contact angle was observed between TPU-0 and TPU-1 (**Figure 16**). However, a high PDMS content would lead to surface segregation of the PDMS chains in the TPU. It was therefore determined that the suitable PDMS content without adversely affecting the surface properties was up to 5 wt%.

Table 8. Values of the ratio of the Si, C : (a) XPS and (b) NMR

(a) XPS ratio of atoms (surface)

PDMS-OH (wt%)	0	1	5	10	20
Si (%)	0	7	12	21	25
C (%)	74	65	59	55	54
Si/C	0	0.11	0.20	0.38	0.46

(b) NMR ratio of atoms (bulk)

PDMS-OH (wt%)	0	1	5	10	20
H (Si-$(CH_3)_2$) (%)	0	3.10	4.17	11.15	19.05
H (CH_2) (%)	42.97	41.39	40.57	31.06	24.25
Si/C	0	0.10	0.10	0.36	0.79
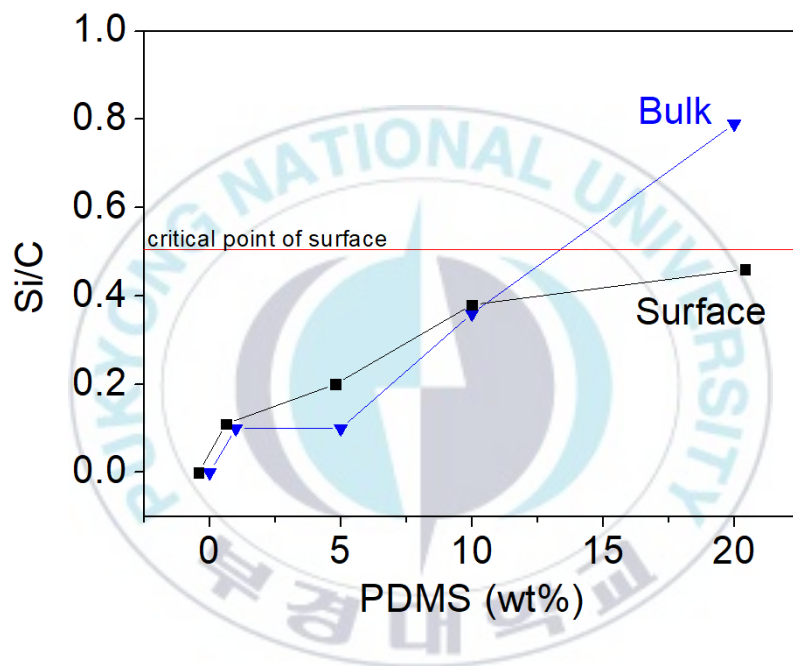
Figure 17. Curves of the Si/C ratio in the XPS and NMR

4.2.5. Mechanical properties

4.2.5.1. Tensile strength & Elongation

Tensile strength and elongation of TPUs with different compositions of PDMS-OH are shown in **Figure 18**. As the PDMS-OH in TPU increases, the elongation increased while the tensile strength sharply decreased at 10 and 20 wt% of PDMS. This is due to the inherent low strength and softness properties of PDMS. The mechanical properties are considered as a reference to the degree of phase separation. The degree of phase separation is related to the level of adhesion between the phases and the ability to transmit stresses across the interface. As the PDMS in the TPU increased, the hydrophobicity increased and the phase separation between hard and soft segments decreased [31, 32]. Thus, the tensile strength with increasing PDMS content in TPU was decreased. However, the tensile strengths of TPUs with 1 and 5 wt% of PDMS were nearly unchanged because small amounts of PDMS do not affect the phase separation.
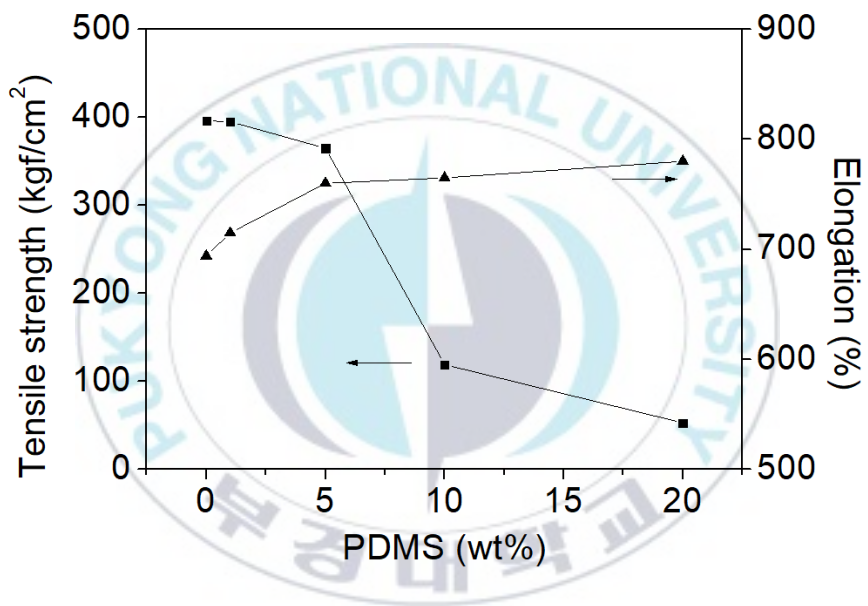
**Figure 18.** Mechanical properties of TPUs with 0, 1, 5, 10, and 20 wt% of PDMS-OH

Table 9. Average values of the tensile strength and Elongation of the TPUs with PDMS-OH wt%

Sample	TPU-0	TPU-1	TPU-5	TPU-10	TPU-20
Tensile strength (kgf/cm²)	396	395	365	119.2	53.1
Elongation (%)	694	715	760	765	780

4.2.5.2. NBS abrasion & Slip resistance

In this paper, the improvement of abrasion resistance with PDMS-OH maintaining slip resistance is the key point. From NBS abrasion resistance in **Figure 19**, the increase of PDMS in TPU leads to increase NBS abrasion resistance. In general, abrasion resistance is affiliated with friction coefficient and so the introduction of PDMS in TPU resulted in the decrease of friction coefficient. The introduction of 5 wt% PDMS in TPU maintains the slip resistance. It indicated that the hydroxyl groups of PDMS-OH reacted to NCO groups and then the migration of PDMS at the surface were prevented. However, the PDMS chains in TPU will be segregated at the surface at high PDMS content.
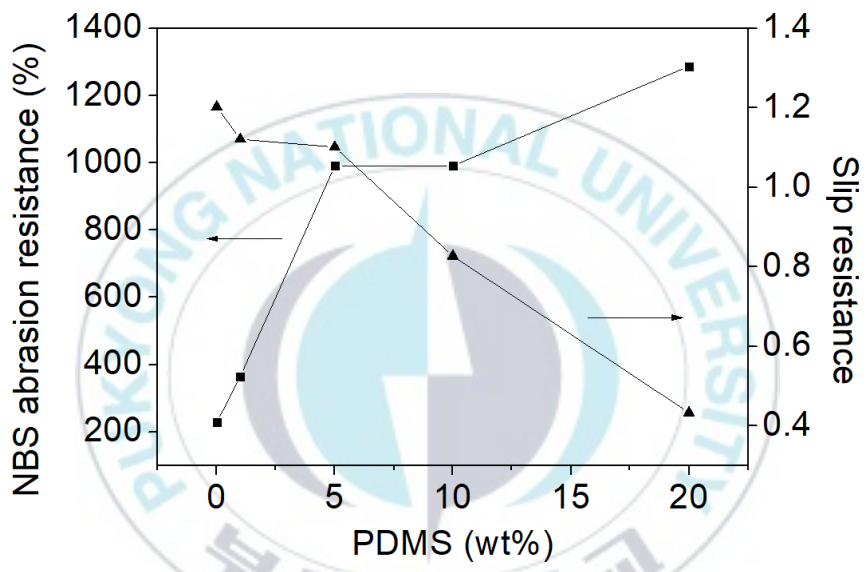
**Figure 19.** NBS abrasion resistance and slip resistance properties of TPUs

Table 10. Average values of the NBS abrasion resistance and slip resistance of the TPUs with PDMS-OH wt%

Sample	TPU-0	TPU-1	TPU-5	TPU-10	TPU-20
NBS abrasion resistance (%)	228	365.2	990.7	991.2	1287.1
Slip resistance	1.202	1.121	1.101	0.827	0.433

4.2.5.3. Rebound resilience

The rebound resilience is an important property to confirm that TPUs are excellent elastomer. The rebound resilience of TPUs is shown in **Figure 20**. In the 0, 1, and 5 wt% of PDMS, the ether groups of TPU much influenced the rebound resilience property because of small amount of PDMS. However, the increase of PDMS content resulted in increasing hydrophobicity. Thus, the degree of phase separation was decreased and the elasticity of TPU decreased [33]. **Figure 21** showed the polylactide (PLA) and TPU-based shoe outsoles produced by 3D printing. Since PLA has been frequently used as a material of 3D printing, the shape and the property of both samples are very similar to each other and then the synthesized TPU can be a candidate for 3D printing materials. As mentioned above, TPUs for 3D printing will be much useful due to easy control of their properties and having property of elastomer.
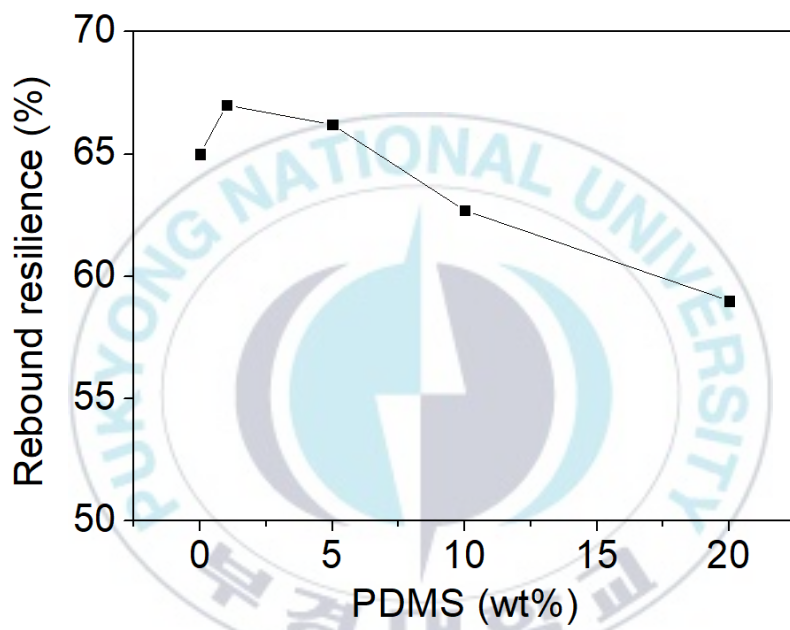
Figure 20. Rebound resilience of TPUs with 0, 1, 5, 10, 20 wt% of PDMS-OH

Table 11. Average values of the rebound resilience of the TPUs with PDMS-OH wt%

Sample	TPU-0	TPU-1	TPU-5	TPU-10	TPU-20
Rebound resilience (%)	65	67	66.2	62.7	59

Figure 21. Samples manufactured by 3D printing: (a) PLA and (b) TPU

5. Conclusions

TPU with hard segment ratio 24 % was suitable for 3D printers because of having excellent mechanical properties and thermal property. but it has low abrasion resistance. In this study, TPUs were synthesized by using hydroxyl-terminated PDMS to increase the abrasion resistance. Elongation and abrasion resistance of TPU were increased while hydroxyl-terminated PDMS increased. However, mechanical properties of TPU with PDMS 10 wt %, 20 wt % were much decreased. Therefore, completely weight ratio of hydroxyl-terminated PDMS was 5%.

6. References

[1] Manners-Bell, J., & Lyon, K. (2012). The implications of 3D printing for the global logistics industry. Transport Intelligence, 1-5.

[2] Ligon, S. C., Liska, R., Stampfl, J., Gurr, M., & Mülhaupt, R. (2017). Chemical reviews, 117(15), 10212-10290.

[3] Stilling, H., & Lin, N. W. (1990). Journal of cellular plastics, 26(6), 475-489.

[4] Voda, A., Beck, K., Schauber, T., Adler, M., Dabisch, T., Bescher, M., ... & Blümich, B. (2006). Polymer testing, 25(2), 203-213.

[5] Vedula, R. R., & Goscewski, S. R. (1999). U.S. Patent No. 5,959,059. Washington, DC: U.S. Patent and Trademark Office.

[6] Krech, R., Mueller, J., Pohlmann, N., Sellig, P., & Steinberger, R. (2003). U.S. Patent No. 6,538,075. Washington, DC: U.S. Patent and Trademark Office.

[7] GRÖNQVIST, R. (1995). Ergonomics, 38(2), 224-241.

[8] Roitman, L., & Auerbach, R. A. (1990). U.S. Patent No. 4,902,767. Washington, DC: U.S. Patent and Trademark Office.

[9] Jiao, L., Zhaoqi, P., & Yun, G. (2007). Journal of applied

polymer science, 105(5), 3037-3046.

[10] Berman, B. (2012). Business horizons, 55(2), 155-162.

[11] Bhushan, B., & Caspers, M. (2017). Microsystem Technologies, 23(4), 1117-1124.

[12] Fischer, F. (2015). Popular Plastics & Packaging, 60(6).

[13] Manoharan, V., Chou, S. M., Forrester, S., Chai, G. B., & Kong, P. W. (2013). Virtual and Physical Prototyping, 8(4), 249-252.

[14] Hiemenz, J. (2011). Stratasys Inc, 1, 1-5.

[15] Kruth, J. P., Wang, X., Laoui, T., & Froyen, L. (2003). Assembly Automation, 23(4), 357-371.

[16] Cai, F., Khan, W. T., & Papapolymerou, J. (2015, May). In 2015 IEEE MTT-S International Microwave Symposium (pp. 1-4).

[17] Sharmin, E., & Zafar, F. (2012). An Introduction. Polyurethane, 3-16.

[18] M. Rogulska, A. Kultys, W. Podkos, 43 (2007) 1402-1414.

[19] Thomas, S., Datta, J., Haponiuk, J., & Reghunadhan, A. (Eds.). (2017). Elsevier.

[20] Hepburn, C. (2012). Springer Science & Business Media.

[21] Buckley, C. P., Prisacariu, C., & Martin, C. (2010). Polymer,

51(14), 3213 – 3224.

[22] J. O. Akindoyo, M. D. H. Beg, S. Ghazali, M. R. Islam, N. Jeyaratnam, and A. R. Yuvaraj (2016), RSC Advances, 6, 114453.

[23] Blackwell, J., & Gardner, K. H. (1979). Polymer, 20(1), 13 – 17.

[24] Ullmann's Encyklopaedie Der Technischen Chemie, 4th Edition, Volume 19, Ed., E. Bartholome, Verlag Chemie, Weinheim, Germany, 1972, p.297-299

[25] P.M. Dreyfuss and M.P. Dreyfuss in Encyclopedia of Polymer Science and Technology, Eds., H.F. Mark, N.G. Gaylord and N.M. Bikales, Volume 13, Interscience, New York, NY, USA, 1970, p.670-691.

[26] J.D. Cox, Tetrahedron, 1963, 19, 7, 1175.

[27] Ionescu, M. (2005). iSmithers Rapra Publishing.

[28] Aitken, R. R. & Jeffs, G. M. F. (1997). Polymer 18, 197-198.

[29] Wang, L. F., Ji, Q., Glass, T. E., Ward, T. C., McGrath, J. E., Muggli, M., ... & Sorathia, U. (2000). Polymer, 41(13), 5083-5093.

[30] Sa'ude, N., Kamarudin, K., Ibrahim, M., & Ibrahim, M. H. I.

(2015). In Applied Mechanics and Materials (Vol. 773, pp. 3-7). Trans Tech Publications.

[31] Ra, S. H., Lee, H. D., Kim, Y. H. (2015). polymer (Korea), 39(4), 579-587.

[32] Rajan, K. P., Al-Ghamdi, A., Ramesh, P., & Nando, G. B. (2012). Journal of Polymer Research, 19(5), 9872.

[33] Mok, D. Y., Shin, H. D., Kim, D. H., Kim, G. N., & Kim, I. S. (2013). Elastomers and Composites, 48(4), 256-262.

[34] Jeong, B. Y., Choi, M. J., Lee, W. K., Chun, J. H., Cheon, J. M., & Ha, C. S. (2018). 660(1), 115-120.

[35] Chun, J. H., Cheon, J. M., Jeong, B. Y., & Lee, W. K. (2017). Molecular Crystals and Liquid Crystals, 653(1), 220-225.

[36] Ngo, T. D., Kashani, A., Imbalzano, G., Nguyen, K. T., & Hui, D. (2018). Part B: Engineering, 143, 172-196.

[37] Chen, L., He, Y., Yang, Y., Niu, S., & Ren, H. (2017). The International Journal of Advanced Manufacturing Technology, 89(9-12), 3651-3660.